

The supernova remnant RX J0852.0–4622: radio characteristics and implications for SNR statistics

A.R. Duncan¹ and D.A. Green²

¹ Max-Planck-Institut für Radioastronomie, Auf dem Hügel 69, D–53121 Bonn, Germany

² Mullard Radio Astronomy Observatory, Cavendish Laboratory, Madingley Road, Cambridge CB3 0HE, U.K.

Received 23 December 1999 / Accepted 31 August 2000

Abstract. We present new radio observations of the recently identified, young Galactic supernova remnant (SNR) RX J0852.0–4622 (G266.2–01.2) made at 1.40 GHz with a resolution of 14′.9. These results, along with other radio observations from the literature, are used to derive the extent, morphology and radio spectrum of the remnant. The possible age and distance to this remnant are discussed, along with the consequences of its properties – especially its low radio surface brightness – for statistical studies of Galactic SNRs. The extended features identified by Combi et al. (1999) are considered, and we conclude that these are probably unrelated to the new remnant. If RX J0852.0–4622 is nearby, as is suggested by the available γ -ray data, then the range of intrinsic radio luminosities for SNRs of the same diameter may be much larger than was previously thought.

Key words: Polarisation – ISM: supernova remnants – Radio continuum: general

1. Introduction

Recently, Aschenbach (1998) reported the discovery of a young supernova remnant (SNR) – designated RX J0852.0–4622 – from high-energy X-ray data from the ROSAT All-Sky Survey. This new SNR appears near the southeastern boundary of the Vela remnant (e.g. Milne 1995; Aschenbach et al. 1995; Duncan et al. 1996), appearing in X-rays (with $E > 1.3$ keV) as a nearly circular “ring” approximately 2° in angular diameter. Around the circumference of this ring are a number of enhancements in the X-ray emission, the most prominent of which appears near the northwestern perimeter. The available X-ray and γ -ray data show the remnant to be comparatively young, with an age of $\lesssim 1500$ yr (Iyudin et al. 1998; Aschenbach et al. 1999).

Following from this X-ray detection, Combi et al. (1999) reported a radio detection of the SNR from the 2.42-GHz data of Duncan et al. (1995). These authors present spatially filtered data from the Parkes 2.42-GHz survey, along with re-

sults obtained from the 30-m Villa Elisa telescope at 1.42 GHz (beamwidth $\sim 34'$).

The possibility of providing a more accurate age for this remnant was raised by Burgess & Zuber (1999), who present a re-analysis of nitrate abundance data from an Antarctic ice core. These authors find evidence for a nearby Galactic SN 680 \pm 20 years ago, in addition to the known historical supernovae (e.g. Clark & Stephenson 1977), although it is not possible to link this new SN definitively with RX J0852.0–4622.

In this paper, we examine three sets of radio continuum data from the Parkes telescope, at frequencies of 1.40, 2.42 and 4.85 GHz. We use these data to further investigate the radio structure of RX J0852.0–4622. Implications of the radio characteristics of this remnant for statistical studies of SNRs are then considered.

2. Radio data

The radio data presented here come from three principal sources, at frequencies of 4.85, 2.42 and 1.40 GHz. Characteristics of these data are given in Table 1.

First, 4.85-GHz data have been obtained from the Parkes-MIT-NRAO (PMN) survey images (Griffith & Wright 1993). These images were observed using the 64-m Parkes radio telescope, and have an angular resolution of approximately $5'$. Processing of the PMN observations has removed large-scale information ($\gtrsim 1^\circ$) from the data. Nevertheless, the PMN images are a useful source of higher resolution information, and are often able to trace structures of large angular size through associated smaller-scale emission components (e.g. Duncan et al. 1997).

Second, 2.42-GHz data surrounding RX J0852.0–4622 have been observed as part of a larger survey presented by Duncan et al. (1995). These data have a resolution of $10'.4$ and include linear polarisation information. Some results from these data pertaining to the Vela region have been presented by Duncan et al. (1996). These data were used by Combi et al. (1999) to make the radio detection of RX J0852.0–4622.

Third, 1.40-GHz observations of the region containing the remnant were obtained in 1996 September, as part of a larger survey of the Vela region at this frequency. Some of these data have already been used by other authors (e.g. Sault et al. 1999).

Table 1. Details of the radio observations of RX J0852.0–4622. Note that the PMN survey data contain no information on scale-sizes of $\simeq 1^\circ$ and larger. The rms noise is quoted per beam area.

Frequency (/GHz)	rms noise (/mJy)	Angular resolution	Stokes	Data origin
1.40	20	14'.9	<i>I, Q, U</i>	this paper
2.42	17	10'.4	<i>I, Q, U</i>	2.42-GHz survey
4.85	8	5'	<i>I</i>	PMN survey

The observing procedure employed for these 1.40-GHz data was analogous to that used for the 2.42-GHz survey (Duncan et al. 1995). The telescope was scanned over a regularly-spaced coordinate grid, at a rate of 6° per minute, until the region of interest had been completely covered. This procedure was then repeated, scanning the telescope in the orthogonal direction. Stokes-*I*, *Q* and *U* data were recorded. The source PKS B1934–638 was used as the primary gain calibrator for the observations. The flux density of this source was assumed to be 14.90 Jy at a frequency of 1.40 GHz. The source 3C138 was also observed, in order to calibrate the absolute polarisation position-angles. The intrinsic polarisation position-angle of 3C138 is 169° (Tabara & Inoue 1980). After the calculation and subtraction of appropriate “baselevels” from each scan, each pair of orthogonally-scanned maps was combined.

3. Location and morphology

The radio emission from RX J0852.0–4622 is superposed upon a highly structured region of the Vela remnant. Much of this confusing emission is of similar surface brightness to that seen from the new SNR. Furthermore, the very bright, thermal region RCW 38 lies almost adjacent to the southeastern boundary of RX J0852.0–4622. The peak flux of RCW 38 is approximately 150 Jy beam^{-1} in the 2.42-GHz data.

The presence of this confusing radio structure, both thermal and non-thermal, meant that RX J0852.0–4622 was not recognised as an SNR from pre-existing radio observations of the region. Prior to the X-ray discovery of RX J0852.0–4622 the non-thermal emission in this region was thought to emanate from the Vela SNR.

3.1. The 2.42-GHz morphology

The filtered 2.42-GHz image presented by Combi et al. (1999) clearly shows the SNR to have a shell-like radio morphology. This is even apparent in unfiltered maps of the region, such as that presented in Fig. 1. Indeed, the emission now known to be associated with RX J0852.0–4622 can be recognised in the radio images presented by Duncan et al. (1995, 1996). Combi et al. (1999) also identify several additional features within their radio image, designated “A” through “D”, which they suggest may represent extensions to the radio shell. These will be considered in more detail in Sect. 3.4. It should be noted that – possibly as a result of their filtering procedure – the 2.42-GHz

image presented by Combi et al. (1999) does not show either the H II region RCW 38, or the bright, non-thermal emission from Vela-X to the west.

Fig. 2 shows a spatially-filtered image of the region surrounding RX J0852.0–4622. This image has been filtered using the “bgf” algorithm (e.g. Sofue & Reich 1979), implemented within the NOD2 software package. A number of filtering resolutions were used, and it was (qualitatively) determined that the emission from RX J0852.0–4622 was optimally enhanced with a filtering resolution of approximately $30'$ to $40'$ (in agreement with Combi et al. 1999).

A filtering resolution of $40'$ was used for the radio data presented in Fig. 2. This figure shows both the emission from RX J0852.0–4622 and the confusing structure more clearly. Comparing Fig. 2 with the unfiltered data presented in Fig. 1, it can be seen that removal of the large-scale structure does not have a major effect on the appearance of the field.

The radio image of the new remnant is dominated by two opposing arcs. Some fainter radio emission is visible on the remnant’s western side, although there is no obvious counterpart to the east. The brightest section of the radio shell lies to the northwest, and appears approximately coincident with the brightest region of the X-ray image. Comparing the radio with the X-ray emission (Fig. 2, lower panel), we see that the distributions of both are generally similar, at least in as much as can be discerned from the cluttered radio field.

3.2. The 4.85-GHz PMN data

Fig. 3 shows data from the 4.85-GHz PMN survey from the same region as shown in the previous figures. Although this survey is not optimised for extended sources, the northern and southern sections of the limb-brightened shell stand out clearly.

The black circle near the centre of Fig. 3 fits the outer boundary of the radio emission from both Figs 2 and 3 well, and represents what we take to be the outer boundary of the radio emission from RX J0852.0–4622. This boundary is 1.8 ± 0.2 in angular diameter, and is centred on the X-ray centre of the SNR (as given by Aschenbach 1998). Within the uncertainties, this diameter is in agreement with that estimated by Combi et al. (1999), who quote a value of 2.1 , based upon the (lower resolution) Parkes 2.42-GHz data alone.

Both the radio and X-ray data are consistent with a remnant centred on Galactic longitude 266.2 , latitude -1.2 . Thus, we suggest a Galactic designation of G266.2–01.2 for this SNR.

3.3. Confusing structure within the field

As can be seen from Fig. 2, a good deal of additional radio structure is visible in the vicinity of RX J0852.0–4622. Over the remnant itself, most of this structure takes the form of two diffuse “filaments”, each of which is $\simeq 20'$ wide. These filaments are oriented approximately north–south over the new

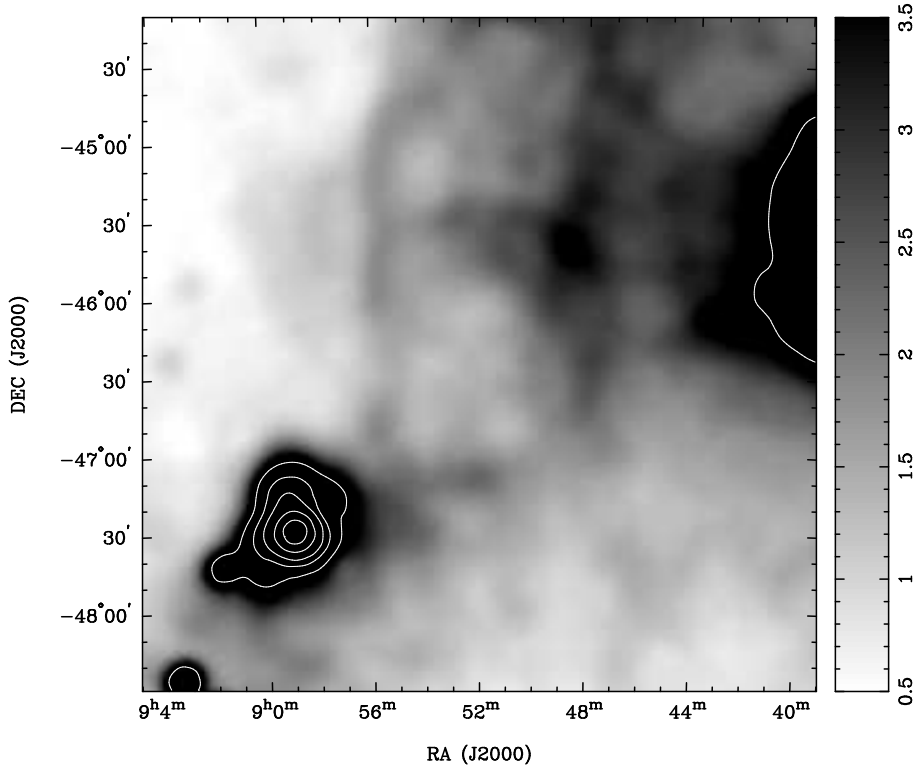


Fig. 1. Unfiltered, Parkes 2.42-GHz survey image of RX J0852.0–4622. Although confused with larger structures, radio emission from the SNR – approximately $1^{\circ}8$ in diameter in the centre of the image – is clearly visible. To the west, the brighter emission associated with Vela-X is visible. To the southeast lies the bright H II region RCW 38. The angular resolution is $10''.4$, and the rms noise is approximately 17 mJy beam^{-1} . The grey-scale wedge is labelled in units of Jy beam^{-1} . Contour levels are: 5, 10, 20, 50 and 100 Jy beam^{-1} .

SNR. Beyond the northern boundary of the remnant, the filaments begin to curve towards the west.

From larger images of the Vela region, such as have been presented by Duncan et al. (1995, 1996), these filaments are known to curve around Vela-X, forming almost a full quadrant of a circle. The eastern arc (as seen in Fig. 2) is highly polarised (e.g. Duncan et al. 1996), and appears to represent the current boundary of the shock from the Vela supernova event.

Interestingly, the confusing filaments from Fig. 2 are almost completely absent from the PMN data. This is because of the observing and data processing procedures used as part of the PMN survey, coupled with the fact that the confusing filaments lie approximately parallel to the scanning direction of the telescope over the region of sky containing RX J0852.0–4622.

3.4. Extensions to the radio shell?

As mentioned in Sect. 3.1, Combi et al. (1999) identify a number of additional features within their radio image. These features were designated “A” through “D” in Fig. 1 of their paper, and apparently extend for relatively large angular distances beyond the edge of the RX J0852.0–4622 shell (up to almost twice the radius of the remnant). Combi et al. (1999) argue that these features may represent extensions to the radio shell of

RX J0852.0–4622 (c.f. Aschenbach et al. 1995). It is of interest to consider these in more detail.

Examining the 2.42-GHz radio image of Combi et al. (1999), we find that radio features “A” and “C” appear to be sections of the much more extensive “arc” structures discussed in Sect. 3.3. These arcs can be traced in Fig. 2 for several degrees, up to the northern edge of the figure (i.e., beyond the boundary of RX J0852.0–4622). Larger radio images of the region show that these features continue for many degrees further, in both total-power and polarised intensity. Feature “B” appears to be an isolated, slightly extended source with no obvious connection to the new remnant (even in the unfiltered image presented in Fig. 1). Finally, feature “D” corresponds to the X-ray feature “D/D’” as identified by Aschenbach et al. (1995). Aschenbach (1998) notes that this feature is also a source of hard X-rays, but that this emission is associated with a much lower temperature spectrum than that from RX J0852.0–4622.

We suggest, therefore, that none of the possible “extensions” identified by Combi et al. (1999) are associated with RX J0852.0–4622.

A further argument against an association between these features and the new remnant is that the boundary of the RX J0852.0–4622 shock is well fitted (in both the PMN and Parkes 2.42-GHz survey data) by a circle. This is consistent with the radio morphologies of other young shell SNRs, such

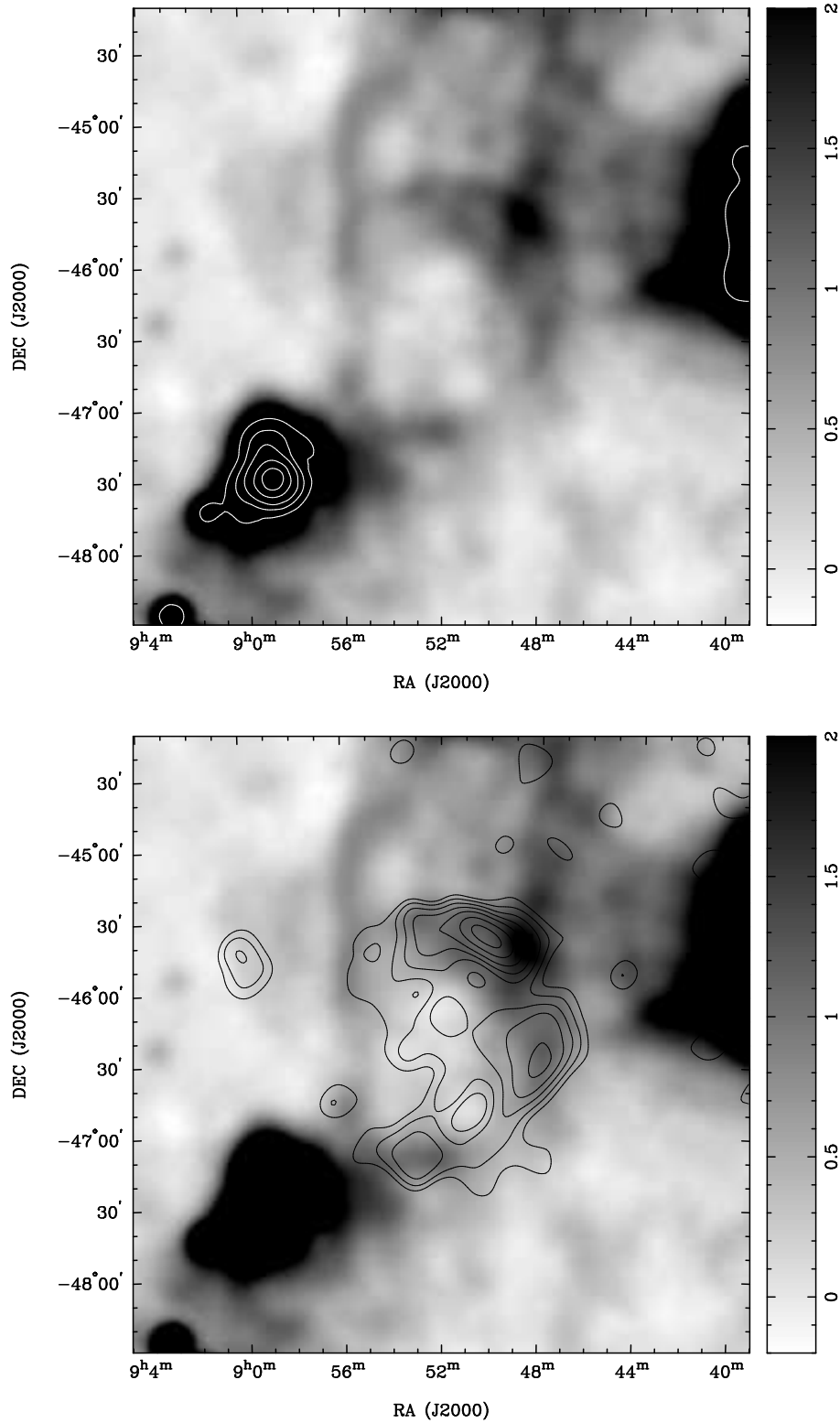


Fig. 2. The optimally-filtered, Parkes 2.42-GHz survey image of RX J0852.0–4622. A filtering beamwidth of 40' has been used, such that larger-scale emission components have been eliminated. The SNR is now more obvious, although it is still heavily confused with emission from the much larger Vela remnant. The angular resolution is 10'4, and the rms noise is approximately 17 mJy beam⁻¹. The grey-scale wedge is labelled in units of Jy beam⁻¹. The upper panel shows radio contours, with levels of: 5, 10, 20, 50 and 100 Jy beam⁻¹. The lower panel shows contours of X-ray intensity – from the 12' resolution images of Snowden et al. (1997) – with levels of: 0.30, 0.40, 0.52, 0.65, 0.80, 1.0 and 1.2 × 10⁻³ counts s⁻¹ arcmin⁻².

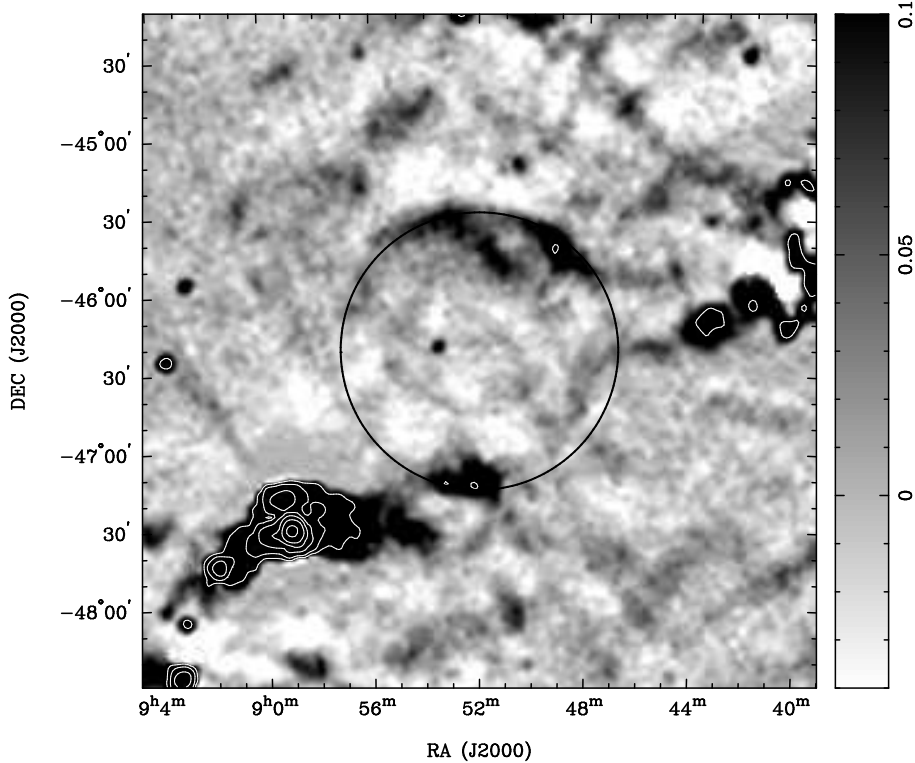


Fig. 3. An image taken from the 4.85-GHz PMN survey, centred on the remnant RX J0852.0–4622. The angular resolution is $\simeq 5'$, and the rms noise is approximately 8 mJy beam^{-1} . The grey-scale wedge is labelled in units of Jy beam^{-1} . The white contours denote intensities of: 0.2, 0.8, 3.0, 10, 30 and 80 Jy beam^{-1} . The black circle (see Sect. 3.2) is centred on the X-ray coordinates of the source and is 1.8 in angular diameter.

as Kepler (Dickel et al. 1988), Tycho (Dickel et al. 1991), and the remnant of SN1006 (Reynolds & Gilmore 1993), although we caution that RX J0852.0–4622 is considerably fainter than these and other young remnants. We also note that the higher resolution PMN image (Fig. 3), although not optimised for extended emission, shows no evidence for any connections between the features noted by Combi et al. (1999) and the shell of the new remnant.

3.5. The quasi-central source

The PMN image shows that a point-like (i.e. unresolved at a resolution of $\simeq 5'$) source lies approximately 15.5 east of the apparent centre of the remnant. This source is not coincident with either of the two compact X-ray sources near the centre of the remnant that are discussed by Aschenbach et al. (1999). The PMN survey source catalogue (Wright et al. 1994) lists this source as PMN J0853–4620, with a 4.85-GHz flux of $136 \pm 11 \text{ mJy}$. Being relatively faint, our ability to detect PMN J0853–4620 in the 2.42-GHz data is compromised somewhat by confusion, coupled with beam dilution. Nevertheless, we can establish the 2.42-GHz flux to be $\lesssim 200 \text{ mJy}$. This leads to a spectral index for this source of $\alpha \gtrsim -0.7$ (with $S \propto \nu^\alpha$).

The radio spectral indices of pulsar emissions are generally much steeper than the $\gtrsim -0.7$ estimated above for the source (e.g. Taylor et al. 1993). Furthermore, a flux of $136 \pm 11 \text{ mJy}$ at a frequency of 4.85 GHz would be exceptionally high for a pulsar. It is much more likely, then, that the PMN J0853–4620 source is extragalactic in origin, rather than associated with RX J0852.0–4622.

3.6. Radio spectrum

The presence of the confusing structure noted in Sect. 3.3 makes accurate estimates of the integrated remnant flux density difficult. The values for the flux density of the SNR given below were estimated by integrating the emission within the boundary of RX J0852.0–4622, as defined by the circle seen in Fig. 3 (lower panel). The integrated area extended approximately one beamwidth beyond this circle, in order to include all the flux from the shell. The base level was determined from flux minima near the centre of the remnant, as well as beyond the eastern and southwestern edges of the shell. Fluxes contributed by the confusing “filaments” seen to the western and eastern sides of the remnant (as discussed in Sect. 3.3) were estimated and subtracted from the total, integrated flux. Note that the uncertainties in the integrated flux values are dominated by

baselevel uncertainty, rather than by uncertainties in the flux estimates of the confusing structure.

We estimate the integrated fluxes of RX J0852.0–4622 at 2.42 and 1.40 GHz to be 33 ± 6 Jy and 40 ± 10 Jy, respectively. These values lead to a very uncertain estimate of the spectral index, with $\alpha = -0.4 \pm 0.5$ ($S \propto \nu^\alpha$). To better establish the spectral index of the remnant, the method of “T–T” plots was used (e.g. Turtle et al. 1962).

Estimates of the remnant spectral index were made from both filtered and unfiltered images, using the T–T plot technique. The northern section of the shell was found to have a consistent, non-thermal index of -0.40 ± 0.15 . The southern section of emission exhibited a much flatter spectrum of -0.1 ± 0.1 . We believe this latter value to be unreliable, due to the proximity of the southern section of the shell to the bright H II region RCW 38 and its associated emission. At the lower angular resolution of the 1.40-GHz data (to which the 2.42-GHz data are also smoothed, for the purposes of spectral index calculation), some of this thermal emission becomes confused with the southern arc of RX J0852.0–4622. We suggest that the value determined for the northern shell section better represents the new remnant’s radio emission.

Extrapolating the measured integrated flux to a frequency of 1 GHz (using a spectral index of -0.40 ± 0.15), we determine a value of 47 ± 12 Jy, leading to an average surface brightness at this latter frequency of $(6.1 \pm 1.5) \times 10^{-22} \text{ W m}^{-2} \text{ Hz}^{-1} \text{ sr}^{-1}$. The above values are summarised in Table 2.

4. Polarimetric observations

We have examined the 1.40- and 2.42-GHz polarimetric data in the field surrounding RX J0852.0–4622. These data have been used to estimate the Faraday rotation measures (RMs) across the field, and to calculate the polarisation position-angles at zero wavelength (thereby estimating the orientations of the tangential components of the magnetic fields within the regions of polarised emission). Note that these estimates assume the polarisation position-angles to vary linearly with λ^2 .

The polarised intensities from the 2.42-GHz data are shown in Fig. 4, at the lower resolution of $14''.9$. Superposed upon this grey-scale image are the orientations of the tangential component of the magnetic field. The RMs derived across the field are shown in Fig. 5.

The large circle shows the boundary of the SNR RX J0852.0–4622. Much of the polarised emission visible within the circle does not appear to be associated with the new SNR. For example, the polarisation detected from the eastern half of RX J0852.0–4622 is clearly associated with the prominent, eastern arc of total-power emission. The only region of RX J0852.0–4622 to potentially exhibit polarised emission is the northern section of the shell. If associated with the new remnant, the northern arc appears polarised to a level of approximately 20% at 2.42 GHz. Other regions of the SNR ex-

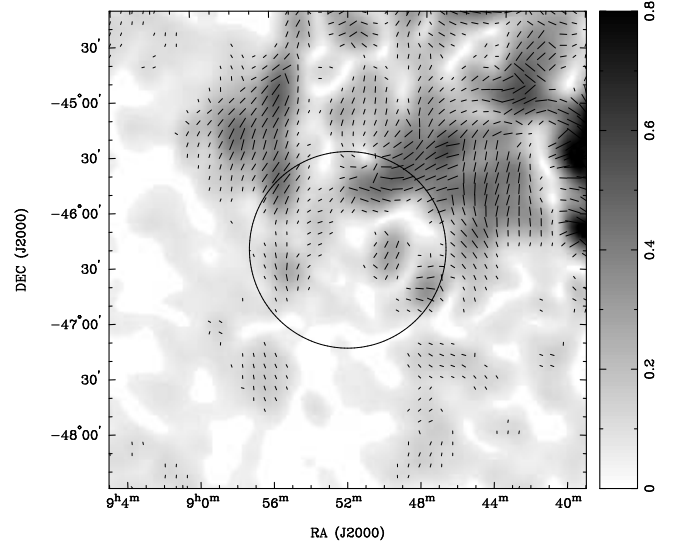


Fig. 4. Grey-scale image showing the polarised intensities across the field at 2.42 GHz, with a resolution of $14''.9$. The 2.42-GHz Stokes- Q and U data have rms variations of $\simeq 23 \text{ mJy beam}^{-1}$ at this resolution. The grey-scale image is blanked wherever the polarised intensity falls below 45 mJy beam^{-1} . Orientations of the tangential components of the magnetic fields are also shown. These angles have been calculated from the 1.40- and 2.42-GHz data, assuming that the vector angles vary linearly with λ^2 . Errors in the derived angles are generally $\lesssim 10^\circ$. A vector is plotted every $6'$, wherever both the 1.40- and 2.42-GHz polarised intensities (at $14''.9$ resolution) exceed 0.1 Jy beam^{-1} . The grey-scale wedge is labelled in units of Jy beam^{-1} .

hibit no polarised emission (such as the southern section of the shell), or are confused with polarised structure from Vela.

The magnetic field vectors on the north side of the shell appear jumbled, with no clear orientation evident. This is in contrast to the field orientations in other young, shell-type supernova remnants, which are predominantly radial; e.g. Tycho (Wood et al. 1992), Kepler (Matsui et al. 1984) and SN1006 (Reynolds & Gilmore 1993).

However, it is questionable whether the detected polarised emission in this northern section of the shell is attributable to RX J0852.0–4622. The appearance of much of this RM structure is similar to that seen from the Vela emission, beyond the RX J0852.0–4622 shell’s northwestern perimeter. Furthermore, there is no discontinuity in either the RM values or the magnetic field orientations near the boundary of the shell. We suggest, therefore, that the polarised emission seen throughout Fig. 4 originates entirely from the Vela remnant. We note that this interpretation is also consistent with the lack of polarisation observed from the southern arc of the RX J0852.0–4622 shell.

The fractional polarisation of the northern arc must then be $< 20\%$ at 2.42 GHz. As noted above, we detect no polarisation in the vicinity of the bright, southern section of the shell, to a (5σ) limit of approximately 5% at 2.42 GHz. We note that these

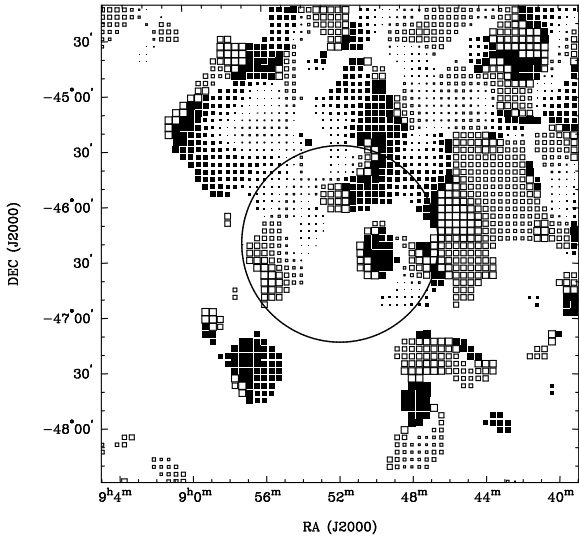


Fig. 5. The derived rotation measure (RM) from the 2.42- and 1.40-GHz data, assuming that the vector angles vary linearly with λ^2 . Filled squares represent positive RM values, while empty squares represent negative values. The size of each square is proportional to the magnitude of the RM, with the maximum size corresponding to $\simeq \pm 51 \text{ rad m}^{-2}$. The errors in RM values are $\lesssim 5 \text{ rad m}^{-2}$. A square is plotted every $4'$. Data have been blanked wherever the 1.40- or 2.42-GHz polarised intensity (at 14.9 resolution) falls below 0.1 Jy beam^{-1} .

Table 2. Characteristics of the radio emission from RX J0852.0–4622, determined from the Parkes data. The spectral index measured for the southern limb of the SNR appears to be confused with nearby thermal emission. The surface brightness is given in units of $\text{W m}^{-2} \text{ Hz}^{-1} \text{ sr}^{-1}$.

Angular diameter	1.8 ± 0.2
Integrated 1.40-GHz flux density	$40 \pm 10 \text{ Jy}$
Integrated 2.42-GHz flux density	$33 \pm 6 \text{ Jy}$
α_{northern} (from T-T plots)	-0.40 ± 0.15
α_{southern} (from T-T plots)	$-0.1 \pm 0.1(?)$
Integrated flux density at 1 GHz	$47 \pm 12 \text{ Jy}$
Surface brightness at 1 GHz	$(6.1 \pm 1.5) \times 10^{-22}$

low fractional polarisations are not inconsistent with the polarimetric properties of other young shells, which exhibit fractional polarisations of $\lesssim 15\%$ when the emission is well resolved.

5. Discussion

5.1. RX J0852.0–4622: young or not so young?

Several observations of RX J0852.0–4622 suggest that it is a young SNR. Most notably, both the X-ray temperatures derived by Aschenbach (1998) and the γ -ray work of Iyudin et al. (1998) imply an age of $\lesssim 1500$ yr. Further, the more recent discussion of the γ -ray observations by Aschenbach et al. (1999) suggest the remnant is ~ 700 years old. This is in

agreement with the approximately circular radio appearance of the remnant; a characteristic exhibited by other young, shell-type SNRs. Even the cautious upper distance limit of approximately 1 kpc provided by Aschenbach (1998), which leads to a linear diameter of $\simeq 30$ pc, implies the age of this remnant cannot be more than a few thousand years.

However, there are some radio properties of this remnant are difficult to reconcile with those of other young SNRs.

- The radio shell is far from complete. The radio image of RX J0852.0–4622 is composed primarily of two, opposing regions of emission. This is in contrast to other young, shell-type SNRs, which exhibit essentially complete radio shells. We note a possible resemblance to the structure of SN1006, however, which also shows opposing arcs of emission.
- The radio emission from this new SNR is of relatively low surface brightness. The mean radio surface brightness of this new remnant at 1 GHz (see Table 2) is a factor of 5 lower than that of SN1006. This is significant, because the SN1006 remnant has the lowest surface brightness of all the young, shell-type SNRs in current catalogues (e.g. Green 1998) – see the further discussion in Sect. 5.3.
- The radio spectral index of -0.40 ± 0.15 determined herein for RX J0852.0–4622 is flatter than those of other young shells, which have indices of $\lesssim -0.6$ (e.g. Green 1988).

It is possible that some of the unusual radio properties of RX J0852.0–4622 may result from the SNR expanding into a hot, low-density region of the interstellar medium; Aschenbach (1998) determines an upper limit to this density of approximately 0.06 cm^{-3} . If so, this would emphasise the role played by environmental effects on the detectability of young radio remnants. Alternatively, this SNR may be just beginning to “turn on” at radio wavelengths, although this scenario may be difficult to reconcile with the very incomplete radio shell.

Further insights into the unusual radio properties of this SNR must await more detailed investigations of the characteristics of both the remnant and the environment into which it is expanding.

5.2. The distance to RX J0852.0–4622

Unfortunately, the distance to RX J0852.0–4622 is highly uncertain. The X-ray data of Aschenbach (1998) provide an upper limit of approximately 1 kpc, based on the lack of absorption, but suggest that the remnant’s distance could be as small as 200 pc. This lower limit is based upon a comparison of the new remnant’s surface brightness with that of SN1006. However, SN1006 is atypically faint for known, young, Galactic SNRs (this is further discussed in Sect. 5.3).

The γ -ray data discussed by Iyudin et al. (1998) and Aschenbach et al. (1999) suggest an age of approximately 700 yr, from a comparison of the observed ^{44}Ti line flux with that expected from SN models, which corresponds to a distance of approximately 200 pc. However, the interpretation of the γ -ray detection requires the assumption of both the supernova shock

velocity and the ^{44}Ti yield. Iyudin et al. (1998) note that increases in either of these quantities will lead to an increase in the derived distance of the remnant.

We have examined 21-cm H I observations in the region of RX J0852.0–4622, from Kerr et al. (1986), in an attempt to find any correlating features. However, since the remnant lies in a complex region in Vela, no associated features in H I could be found.

The ice core data of Burgess & Zuber (1999) may be able to provide an accurate age for RX J0852.0–4622, but these data are not able to constrain the distance to the SNR without further assumptions. Furthermore, as noted above, it is not possible to definitively associate the additional nitrate spike with this SNR. If we assume the age of $\simeq 700$ yr determined by Burgess & Zuber (1999) to be accurate, then assuming an upper limit to the mean shock velocity of 10^4 km s^{-1} places the remnant at a distance of $\lesssim 460$ pc, with a linear diameter of $\lesssim 15$ pc.

A value of 10^4 km s^{-1} was nominated as an upper limit to the shock velocity by Aschenbach et al. (1999), based on their analysis of the X-ray data. Should the mean shock velocity exceed this value, the remnant would lie at a distance of $\gtrsim 460$ pc, with a correspondingly larger linear diameter.

In summary, the distance is very poorly constrained by current observational data. Unfortunately, since the remnant is faint, is not detected optically, and is in a complex region, many direct techniques used to determine the distance to SNRs are not applicable in this case (e.g. H I absorption, association with other H I features or molecular clouds, or optical studies). Nevertheless, the radio properties of this remnant, even with the present uncertainty in its age and size, have some interesting implications for statistical studies of Galactic SNRs, which are discussed in the next section.

5.3. Statistical implications

Fig. 6 shows a surface-brightness versus diameter plot for Galactic SNRs for which there are reasonable distances available (Green 1984, 1991, 1998). RX J0852.0–4622 is plotted on this figure with a range of diameters corresponding to distances from 200 pc to 1 kpc. The surface brightness of RX J0852.0–4622, of $\Sigma_{1 \text{ GHz}} \sim 6 \times 10^{-22} \text{ W m}^{-2} \text{ Hz}^{-1} \text{ sr}^{-1}$, is faint for a known Galactic SNR – among the faintest 20% of catalogued remnants. This is less than the nominal completeness limit of many radio surveys (e.g. Green 1991). Note that although most faint remnants are thought to be old, that the remnant of the SN of AD1006 is also faint, with $\Sigma_{1 \text{ GHz}} \sim 3 \times 10^{-21} \text{ W m}^{-2} \text{ Hz}^{-1} \text{ sr}^{-1}$. We also note that, whilst RX J0852.0–4622 is one of the fainter remnants to appear on the $\Sigma - D$ plot, the only other remnant detected in ^{44}Ti γ -ray emission is Cas A, which has the highest surface brightness.

From Fig. 6, it is clear that the properties of RX J0852.0–4622 are very unusual if it lies at the smaller distances suggested by the γ -ray data. If the SNR is at a distance < 300 pc, its diameter is less than 10 pc, but its surface brightness is two or more orders of magnitude less than other known young SNRs with similar diameters (e.g. Kepler’s SN, Tycho’s SN,

and 3C58). This would have important consequences for statistical studies of Galactic SNRs (see Green 1991), as the range of Σ – or, equivalently, luminosity – for a given D may be even wider than was previously thought. This in turn would imply that the observational selection effect of faint SNRs being difficult to detect is important, not only for old SNRs, but also for young SNRs. The low radio surface brightness of RX J0852.0–4622 indicates that a fraction of young SNRs may be faint at radio wavelengths. The available sample of young SNRs (i.e. historical events) is small, however, so it is not possible to meaningfully estimate this proportion.

On the other hand, if the remnant is as distant as 1 kpc, then although it is faint for its diameter of ~ 30 pc, it is not strikingly unusual.

6. Conclusions

We have presented various radio observations of the newly recognised SNR RX J0852.0–4622, which clarify its size and morphology. Several features possibly associated with the remnant by Combi et al. (1999) are examined, and it is concluded that these are probably unrelated to RX J0852.0–4622.

Although the distance and age of RX J0852.0–4622 are not well determined, its faintness has some interesting implications for the statistical study of SNRs, namely that the surface-brightness limits of current radio surveys may miss faint, young remnants, as well as faint, old remnants. Clearly an accurate distance determination for this SNR is important, although this is difficult, given its faintness and the fact that it lies in a complex region of the sky, confused with emission from the much larger Vela SNR.

Acknowledgements. The Australia Telescope is funded by the Commonwealth of Australia for operation as a National Facility managed by CSIRO. ARD is an Alexander von Humboldt research Fellow and thanks the Stiftung for their support. The authors gratefully acknowledge P. Slane for helpful comments and suggestions on the manuscript.

References

- Aschenbach B., 1998, *Nat* 396, 141
- Aschenbach B., Egger R., Trumper J., 1995, *Nat* 373, 587
- Aschenbach B., Iyudin A.F., Schönfelder V., 1999, *A&A* 350, 997
- Burgess C.P., Zuber K., 1999, *New Scientist* 163, 2204 (Sept. 18), p. 7
- Clark D.H., Stephenson F.R., 1977, *“The Historical Supernovae”* (Pergamon, London)
- Combi J.A., Romero G.E., Benaglia P., 1999, *ApJ* 519, L177
- Dickel J.R., Sault R., Arendt R.G., Korista K.T., Matsui Y., 1988, *ApJ* 330, 254
- Dickel J.R., van Breugel W.J.M., Strom R.G., 1991, *AJ* 101, 2151
- Duncan A.R., Stewart R.T., Haynes R.F., Jones K.L., 1995, *MNRAS* 277, 36
- Duncan A.R., Stewart R.T., Haynes R.F., Jones K.L., 1996, *MNRAS* 280, 252
- Duncan A.R., Stewart R.T., Haynes R.F., Jones K.L., 1997, *MNRAS* 287, 722

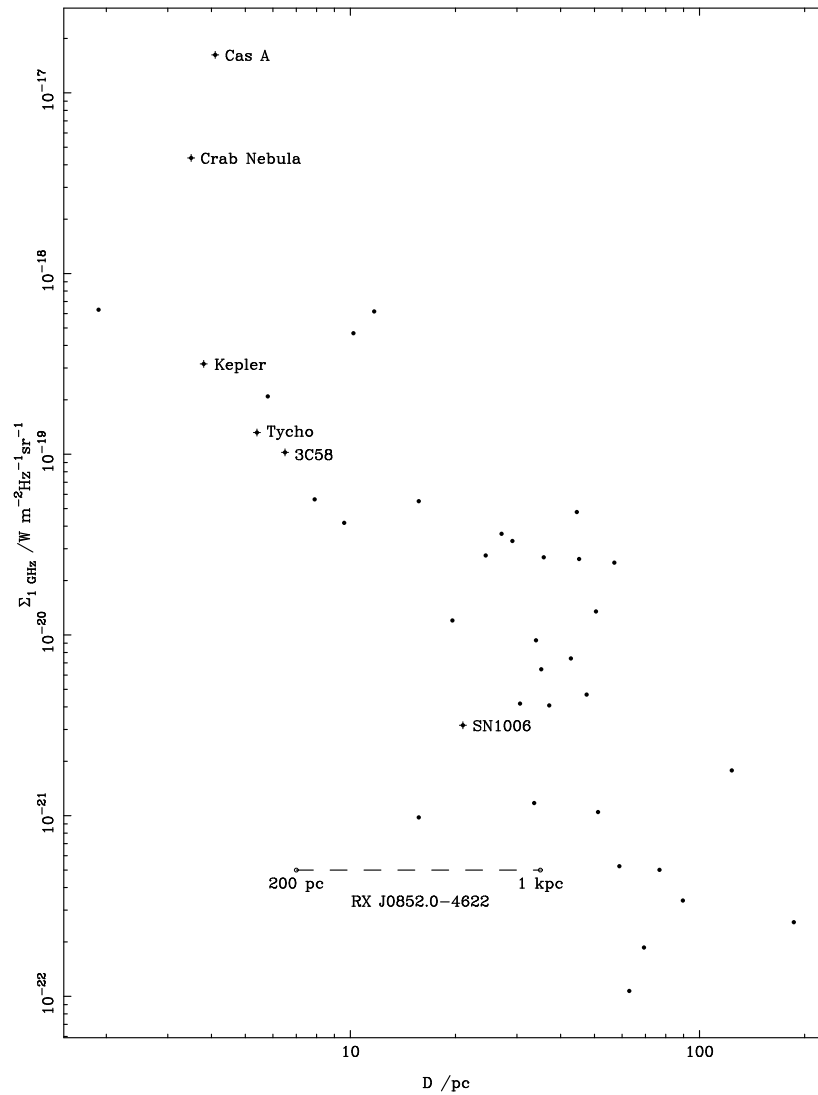


Fig. 6. A surface-brightness vs. diameter ($\Sigma - D$) plot for Galactic SNRs with relatively well known distance. RX J0852.0–4622 is plotted for a range of distances from 200 pc to 1 kpc, and known young SNRs are labelled.

Green D.A., 1984, MNRAS 209, 449

Green D.A., 1988, in “*Genesis and propagation of cosmic rays*”, eds M.M. Shapiro, J.P. Wefel, p. 205 (Reidel, Dordrecht)

Green D.A., 1991, PASP 103, 209

Green D.A., 1998, ‘*A Catalogue of Galactic Supernova Remnants (1998 September version)*’, Mullard Radio Astronomy Observatory, Cambridge, United Kingdom (available on the World-Wide-Web at “<http://www.mrao.cam.ac.uk/surveys/snrs/>”)

Griffith M.R., Wright A.E., 1993, AJ 105, 1666

Iyudin A.F., Schönfelder V., Bennett K., et al., 1998, Nat 396, 142

Kerr F.J., Bowers P.F., Kerr M., Jackson P.D., 1986, AA&S 66, 373

Matsui Y., Long K.S., Dickel J.R., Greisen E.W., 1984, ApJ 287, 295

Milne D.K., 1995, MNRAS 277, 1435

Reynolds S.P., Gilmore D.M., 1993, AJ 106, 272

Sault R.J., Bock D.C.-J., Duncan A.R., 1999, A&AS 139, 387

Schönfelder V., Bloemen H., Collmar W., et al., 2000, ^{44}Ti Gamma-Ray Line Emission from Cas A and RXJ0852.0–4622 / GROJ0852–4642. In: Proc. 5th Compton Symposium (AIP, in press)

Snowden S.L., Egger R., Freyberg M.J., et al., 1997, ApJ 485, 125

Sofue Y., Reich W., 1979, A&AS 38, 251

Tabara H., Inoue M., 1980, A&AS 39, 379

Taylor J.H., Manchester R.N., Lyne A.G., 1993, ApJS 88, 529

Turtle A.J., Pugh J.F., Kenderdine S., Pauliny-Toth I.I.K., 1962, MNRAS 124, 297

Wood C.A., Mufson S.L., Dickel J.R., 1992, AJ 103, 1338

Wright A.E., Griffith M.R., Burke B.F., Ekers R.D., 1994, ApJS 91, 111

Note added in proof: The authors note a recent paper by Schönfelder et al. (2000), which concludes that the γ -ray detection of RX J0852.0–4622 is less statistically significant than was first thought.